

Taylor & Francis
Taylor & Francis Group

Computer Methods in Biomechanics and Biomedical Engineering

ISSN: (Print) (Online) Journal homepage: www.tandfonline.com/journals/gcmb20

Neuro-fuzzy model for predicting insulin delivery from crosslinked agar-carbomer hydrogels

Hadjer Goudjil, Samia Rebouh & Mounir Bouhedda

To cite this article: Hadjer Goudjil, Samia Rebouh & Mounir Bouhedda (07 Jun 2024): Neuro-fuzzy model for predicting insulin delivery from crosslinked agar-carbomer hydrogels, Computer Methods in Biomechanics and Biomedical Engineering, DOI: 10.1080/10255842.2024.2362863

To link to this article: https://doi.org/10.1080/10255842.2024.2362863


Published online: 07 Jun 2024.


Submit your article to this journal


View related articles


View Crossmark data

Full Terms & Conditions of access and use can be found at
https://www.tandfonline.com/action/journalInformation?journalCode=gcmb20

COMPUTER METHODS IN BIOMECHANICS AND BIOMEDICAL ENGINEERING
https://doi.org/10.1080/10255842.2024.2362863

Taylor & Francis
Taylor & Francis Group

Check for updates

Neuro-fuzzy model for predicting insulin delivery from crosslinked agar-carbomer hydrogels

Hadjer Goudjil[a], Samia Rebouh[a,b] and Mounir Bouhedda[c]

[a]Laboratory of Biomaterials and Transport Phenomena (LBPT), Faculty of Technology, University of Medea, Pôle Campus, Medea University, Medea, Algeria; [b]Faculty of Sciences, University of Medea, Ouzera Campus, Medea University, Medea, Algeria; [c]Laboratory of Advanced Electronic Systems (LSEA), Faculty of Technology, University of Medea, Pôle Campus, Medea University, Medea, Algeria

ABSTRACT

This study focuses on the innovation of an inhaled sustained release form of insulin and the development of a neuro-fuzzy model specifically tailored to predict insulin release kinetics from polycondensed agar-carbomer hydrogels. These were synthesized by blending agar and carbomer, incorporating propylene glycol and glycerol, and then cross-linking by polycondensation. The structure and morphology of the hydrogel were analyzed *via* Fourier Transform Infrared Spectroscopy, Scanning Electron Microscopy and Proton Nuclear Magnetic Resonance Spectroscopy. The neuro-fuzzy model, a combination of artificial neural networks and fuzzy logic, employs inputs such as concentrations of crosslinking agents, polycondensation time, and release time, with the output being the rate of insulin release. The model demonstrated a strong correlation with experimental data, highlighting its effectiveness and precision in predicting insulin delivery from hydrogel compositions and temporal parameters. This emphasizes the importance of intelligent modelling for forecasting the kinetic release of therapeutic agents from novel drug delivery systems.

ARTICLE HISTORY
Received 2 November 2023
Accepted 28 May 2024

KEYWORDS
Neuro-fuzzy modeling; hydrogels; insulin delivery; polycondensation; drug release kinetics

1. Introduction

Diabetes is a prevalent chronic condition characterized by the body's inability to maintain physiological blood glucose levels, either due to lack of insulin production in the pancreas or resistance of cells to respond to insulin (Elshaarani et al. 2018). Insulin, a peptide hormone comprising 51 amino acids, was discovered a century ago and remains the primary treatment for diabetes (Mathieu et al. 2021). The extraction, development of analogues, and formulation of insulin from animals and humans have been investigated (Owens et al. 2003; Crasto et al. 2016; Jarosinski et al. 2021). While conventional administration involves multiple daily subcutaneous injections using syringes, issues like absorption variability and patient discomfort have driven research into non-invasive sustained release methods, like inhaled insulin *via* hydrogels (Owens et al. 2003; Baghban Taraghdari et al. 2019). Hydrogels are crosslinked systems of natural or synthetic hydrophilic polymers dissolved in water at low concentrations with a gelling agent (Lefnaoui and Moulai-Mostefa 2013). This forms three-dimensional networks that trap water, yielding translucent semisolids (Lefnaoui and Moulai-Mostefa 2013). Chemical hydrogels are crosslinked by covalent bonds between chains using molecules like polymers or enzymes, conferring durability versus physical hydrogels (Parhi 2017). The crosslinking enables control of drug diffusion and release (Hoare and Kohane 2008). As aerosols, hydrogels are ideal for deep lung delivery, overcoming deposition issues in the mouth and upper respiratory tract (Alsarra et al. 2009). However, reproducible dosing despite respiratory variations remains challenging (Alsarra et al. 2009).

This study addresses the complex task of optimizing hydrogel properties to balance deep lung delivery, dose sufficiency, and respiratory response, though potentially transformative for diabetes Through the synthesis of chemically crosslinked hydrogels using small molecules to link polymer chains, the research aims to fine-tune insulin release kinetics (Parhi 2017; Kaur et al. 2018; Pramanik et al. 2021; Salawi et al. 2022). Inhaled sustained release, if successful, could revolutionize diabetes treatment by enhancing convenience, absorption, and reproducibility compared to traditional subcutaneous injections, while mitigating associated discomfort (Owens et al. 2003; Alsarra et al. 2009; Kankala et al. 2018;

CONTACT Mounir Bouhedda bouhedda.m@gmail.com
© 2024 Informa UK Limited, trading as Taylor & Francis Group

Baghban Taraghdari et al. 2019; Collins et al. 2020; Kumbhar et al. 2022).

The significance of this research lies in its potential to overcome existing challenges in diabetes treatment (Boscari and Avogaro 2021). The development of a reliable and efficient inhaled sustained release system has the capacity to transform patient experiences and treatment outcomes. By mitigating issues associated with subcutaneous injections, such as discomfort and variability, this innovative approach could improve patient adherence and overall quality of life. Furthermore, the exploration of chemically crosslinked hydrogels introduces a novel avenue for controlled drug release, addressing the limitations of current delivery methods (Mansoor et al. 2021).

ANFIS modeling combining neural networks and fuzzy logic has proven effective for investigating pharmaceutical systems (Hezaveh et al. 2012; Zarei and Taheri 2016; Bouhedda et al. 2019; Rebouh et al. 2019). It can analyze complex variable relationships and adapt to uncertain, nonlinear data (Rebouh et al. 2016; Dadkhah et al. 2017; Benyezza et al. 2021; Elbeltagi et al. 2023; Benyezza et al. 2023), optimizing chemical processes by predicting favorable conditions (Kumar 2020). This study uses ANFIS to predict insulin release from an agar-carbomer hydrogel synthesized *via* microwave polycondensation (Hezaveh et al. 2012; Zarei and Taheri 2016; Rebouh et al. 2019). The Adaptive Neuro-Fuzzy Inference System (ANFIS) model was trained on experimental release data from varied hydrogel compositions, then tested on new data. ANFIS shows promise for gaining insights into hydrogel drug delivery despite complex nonlinear dynamics. Its adaptability could allow optimized hydrogel design for enhanced insulin delivery, overcoming limitations in diabetes treatment (Dadkhah et al. 2017; Elbeltagi et al. 2023; Kumar 2020).

The synthesis of chemically crosslinked hydrogels serves as a pivotal starting point in this research, where small molecules are strategically employed to enhance insulin release kinetics. The application of microwave polycondensation takes center stage in the production of agar-carbomer hydrogels, providing a detailed methodology that underlines its significance in optimizing hydrogel properties. Moving on to the characterization phase, this segment delves into the verification of cross-linking through Fourier Transform Infrared (FTIR) spectroscopy. Furthermore, the hydrogel's morphology is meticulously scrutinized using Scanning Electron Microscopy (SEM), offering insights into its structural intricacies, and its crosslinking chemical structure has been elucidated throw Proton Nuclear Magnetic Resonance Spectroscopy (H1NMR). The study then progresses to *In Vitro* Drug Release Modeling using High-Performance Liquid Chromatography (HPLC), where the Korsmeyer-Peppas model has been used to simulate and analyze insulin release dynamics from the synthesized hydrogel. This section contributes a quantitative understanding of the drug release profile, aiding in the assessment of the hydrogel's potential for controlled insulin delivery. Introducing an innovative aspect, the research incorporates ANFIS modeling to predict and optimize insulin release. The ANFIS model is trained with diverse experimental data, showcasing its adaptability, and subsequently, its predictive capabilities are evaluated using new, untrained data. The ensuing discussion critically analyzes the findings to underscore its unique contributions and advantages. The conclusion serves as a platform to suggest avenues for future research, emphasizing the potential for further advancements in hydrogel-based insulin delivery systems.

The rest of this paper is structured as follows. The materials and methods section outlines the synthesis and characterization processes. Results and discussions section covers the detailed analyses of FTIR, SEM and NMR data, as well as insights from Korsmeyer-Peppas and ANFIS modeling. The impact of formulation parameters on insulin release kinetics is examined, with a specific focus on glycerol and propylene glycol concentrations, PG/Gly ratio, and polycondensation time. The conclusion summarizes key findings and their implications, providing a foundation for future research in this area.

2. Materials and methods

In this section, we detail the materials and methods employed in the study, encompassing hydrogel synthesis and drug loading, as well as the comprehensive characterizations conducted through FTIR, SEM and NMR analyses. The hydrogel's drug release kinetics are systematically investigated using Korsmeyer-Peppas Kinetic Modeling, providing a fundamental understanding of the release mechanism. Furthermore, we explore the application of Neuro-Fuzzy Modeling to elucidate the intricate dynamics of drug release kinetics, enhancing our comprehension of the hydrogel's performance in drug delivery applications. The combined utilization of these methodologies ensures a thorough analysis of the synthesized hydrogel's structure, composition, and drug release behavior.

2.1. Materials

Agarose (Ag) and carbomer (Ca) were donated by Orkila (Algeria). The insulin glargine solution was provided by Sanofi (Algeria). Propylene glycol (PG), glycerol (Gly), triethylamine (TEA), sodium chloride, disodium phosphate, potassium phosphate monobasic and potassium chloride were purchased from Sigma-Aldrich (Germany).

2.2. Methods

2.2.1. Hydrogel synthesis and drug loading

The hydrogel was prepared through a microwave-assisted polycondensation reaction between two polymers: carbomer (Ca) and agarose (Ag), along with cross-linking reagents – propylene glycol (PG) and glycerol (Gly). This was carried out according to the method outlined by Santoro et al. (2011), with some minor modifications. To start, 1 g of Ca was dissolved in 100 ml of Phosphate-Buffered Saline (PBS) solution (pH = 7.4), which is a solution commonly used in biological and chemical research to maintain the pH of a solution and mimic the ion concentration of the human body. PBS solution contained Gly and PG at a determined concentration. After that, Triethylamine (TEA), a commonly used organic base in chemistry, was added gradually until the solution reached neutral pH.

Subsequently, 1 gr of Ag was added to the above solution, which was kept at 80 °C under magnetic stirring, and the mixture was left to rest at room temperature. The mixture was then left to rest at room temperature before undergoing a fixed microwave irradiation of 300 W using a Samsung MS23F301TAW SOLO microwave oven. The hydrogels were then formulated and left at room temperature for 24 h.

The insulin glargine-based solution was then added to the polymeric system that had been prepared earlier using a volumetric ratio of 50/50 v/v. The hydrogel compositions of the formulations that were tested can be found in Table 1.

2.2.2 Hydrogels characterizations using Fourier transform infrared spectroscopy (FTIR)

FTIR analysis was carried out on the polymers and hydrogels using a Bruker Tensor II FTIR spectrometer. The spectra were recorded in the wavenumber range of 4000–400 cm^{-1}.

Table 1. Composition of insulin-loaded hydrogel formulations.

Hydrogel formulas	[PG] (%)	[Gly] (%)	PT: Polycondensation time (s)
F1	1	0	0
F2	0	1	10
F3	0	1	30
F4	0	2	20
F5	30	0	10
F6	30	0	20
F7	30	0	30
F8	30	1	10
F9	30	1	20
F10	30	1	30
F11	30	2	10
F12	30	2	30
F13	60	0	20
F14	60	1	10
F15	60	1	30
F16	60	2	20

2.2.3 Scanning electron microscopy (SEM)

The structure and morphology of the Agar-Carbomer hydrogels were examined and visualized using a scanning electron microscope (SEM) with the environmental instrument (ESEM-FEI QUANTA 250) at CRAPC in Algeria. After desiccation in a vacuum oven, the samples were assessed at a voltage of 10 kV and a magnification of ×3000 (Baysal et al. 2013).

2.2.4 Proton nuclear magnetic resonance spectroscopy (NMR)

The Bruker Avance III HD spectrometer, operating at a proton frequency of 400 MHz, was used to analyze polymers, cross-linking systems, and hydrogels. The spectrometer was equipped with a 5 mm diameter liquid broadband probe (BBO) and set to observe nuclei between 31 P and 15 N for the internal coil. The external coil was adjusted to H1 for decoupling and simultaneous observation. Prior to NMR analysis, it is necessary to chemically depolymerize the agar by using hydrogen peroxide in an alkaline solution to reduce the viscosity of the aqueous solution. 7.4 µL NaOH (1 M) and 25 µL H2O2 are added to 1.5 mL of a 6 g/L agar solution in D2O. The solution is stirred and heated to 80 °C for 1 h, then cooled in an ice bath for 30 min before drying. The samples under analysis were dissolved in deuterated solvent D2O. Specifically, 10 mg of each sample was dissolved in 500 µl of the solvent and placed in a 5 mm diameter borosilicate glass NMR tube. The 1H spectra were acquired using the following conditions: Pulse program zg 30°, TD:65536, Acquisition time: 4 sec, Rga:181, DE: 6 u sec, Spectral width: 20 ppm, Number of scans NS =128 scan, P1: 9 u sec and PLW1: 18.86 W.

2.2.5 Korsmeyer-Peppas kinetic modeling of drug release

The kinetic experiment followed the procedure specified in the European Pharmacopoeia (European Pharmacopoeia: 8.0 2014). The hydrogel samples containing the drug were loaded into a polypropylene bag and placed in the basket of a Sotax AT7 dissolution tester. A dissolution medium of 900 ml, PBS 7.4 was added to the rotating cylinder, and the system was maintained at 37 °C with a rotation speed of 50 rpm. 5 mL samples were regularly collected from the dissolution medium every hour for chromatographic analysis using the Waters Alliance 2695 HPLC at a wavelength of 214 nm. An equal volume of fresh PBS 7.4 solution was added to maintain a constant volume.

The *in vitro* insulin release study from a hydrogel, conducted using a Sotax AT7 dissolution tester and analyzed through HPLC, involves a controlled laboratory experiment to mimic and measure the release of insulin from the hydrogel under specified conditions. Consequently, an ANFIS model is used in order to predict and optimize the insulin release. The ANFIS model is trained with diverse experimental data. Figure 1 depicts the *in vitro* insulin release study conducted using a hydrogel.

The Korsmeyer-Peppas model equation is often used to describe drug release kinetics from pharmaceutical dosage forms. The equation is commonly cited in the context of drug delivery and release studies. One of the key references for the Korsmeyer-Peppas model is the original paper by Korsmeyer, Gurny, Peppas. It is given by Equation (1) (Korsmeyer et al. 1983):

$$\frac{M_t}{M_\infty} = kt^n \tag{1}$$

M_t/M_∞ being the released drug rate, k is the kinetic constant, n is an exponent indicating the release mechanism. When $n = 0.43$, Fickian controlled release happens, when $0.43 < n < 0.85$, anomalous transport that refers to cases where the drug release behavior cannot be accurately described using traditional models of diffusion, such as Fick's law, and when $n = 0.85$, this indicates transport relaxation/erosion during drug release, which is the process of drug release caused by the deformation and relaxation of the polymeric network, and can ultimately result in a time-dependent release profile.

2.2.6 Neuro-fuzzy modeling for drug release kinetics

This study proposes an ANFIS model to predict pharmaceutical properties, which is renowned for effectively modeling complex data sets (Rebouh et al. 2016; Bouhedda et al. 2019). Fuzzy logic assesses relationships between uncertain input variables x and output membership functions μ ranging from 0 to 1 (Rebouh et al. 2019). Fuzzy "if-then" rules take the format "if x is A, then y is C" where A and C are linguistic values defined by membership functions like triangular, trapezoidal, or Gaussian (Rebouh et al. 2019; Abba et al. 2020). ANFIS combines fuzzy logic and neural networks to model nonlinear pharmaceutical systems like hydrogels for optimized drug delivery, overcoming limitations in current treatment methods.

$$A = \{x, \mu_a(x)/x \in X\} \tag{2}$$

The model elements of a fuzzy inference system are shown in Figure 2.

The ANFIS model contains a knowledge base of if-then fuzzy rules defining membership functions (Takagi and Sugeno 1985; Huang and Hahn 2009). It fuzzifies crisp inputs into degrees of linguistic values, executes inference on rules, then defuzzifies results into a crisp output. This study uses a first-order Takagi-Sugeno model, suitable for adaptive modeling combined with neural networks to predict

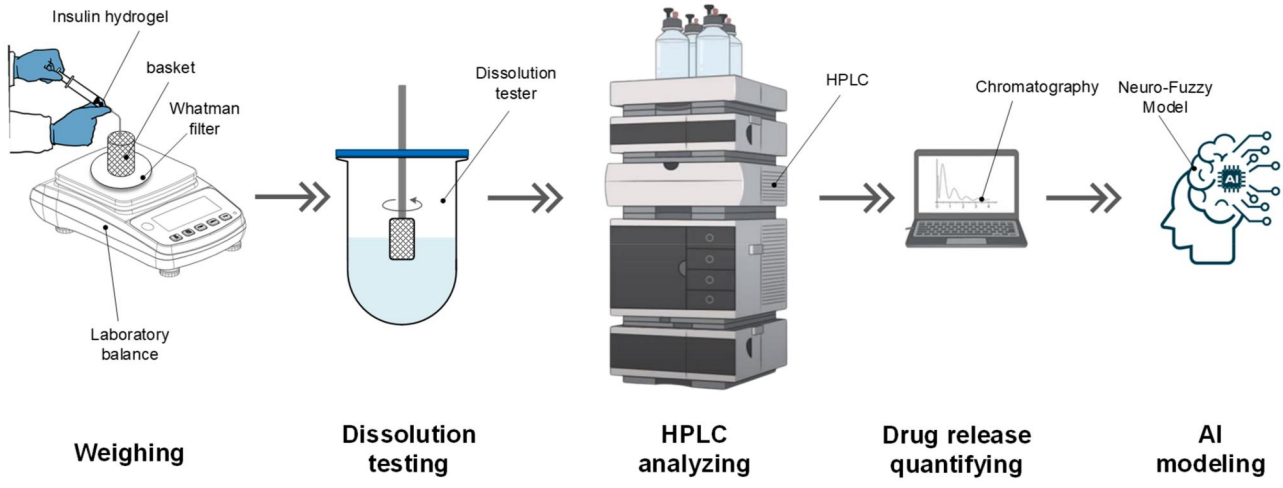


Figure 1. *In vitro* study illustration.

properties of complex systems.

$$\text{If} \quad x_1 \text{ is } A_1 \text{ and } x_2 \text{ is } A_2 \text{ and } x_3 \text{ is } A_3 \text{ then} \\ y = f(x_1,\ x_2,\ x_3) \tag{3}$$

A_1, A_2 and A_3 are fuzzy sets in the antecedent, y is a crisp function in the consequent. A fuzzy inference known as first-order Sugeno fuzzy model occurs when $f(x,y)$ is a first-order polynomial (Figure 3). Particularly, a zero-order Sugeno fuzzy model is obtained when $f(x,y)$ is a constant.

2.2.6.1 ANFIS architecture. The architecture of ANFIS is illustrated in Figure 4. Circular nodes represent the fixed operation, while square nodes portray functions with learnable parameters.

There are five layers in the ANFIS where the function can be explained in the following way (Rebouh et al. 2016).

Layer 1: The fuzzification process occurs in this layer where all the nodes are adaptive. The outputs of this layer constitute the membership values of the assumption part. Each node's output was given by Equation (4):

$$O_{1,i}(x) = \mu_{A_i}(x) \ \text{ for } \ i = 1,2 \\ O_{1,i}(y) = \mu_{B_i}(x) \ \text{ for } \ i = 3,4 \tag{4}$$

$O_{1,i}(x)$ and $O_{1,i}(y)$ are the membership functions for x and y, respectively.

The Gaussian 2 function, given by Equation (5) was used because it gives better results according to Table 2.

$$\mu_A(x) = e^{\frac{-(x-c)^2}{2\sigma^2}} \tag{5}$$

Where σ is the standard deviation and c represents the mean.

Layer 2: each node output is a weight of the rule and all the nodes are here fixed. This is where the t-norm is used to "AND" membership grades as given Equation (6).

$$O_{2,i} = w_i = \mu_{A_i}(x)\mu_{B_i}(y) \ \text{ for } \ i = 1,2 \tag{6}$$

Layer 3: In this layer the nodes are also fixed. The ratio between the firing weight of the i^{th} and the sum of all rule weights is calculated for the corresponding node. It contains fixed nodes which compute the ratio of the firing strengths of the rules according to Equation (7).

$$O_{3,i} = \bar{w}_i = \frac{w_i}{w_1 + w_2} \tag{7}$$

Layer 4: The nodes run as a function block in this layer, with its parameters being adaptive and variables (input values). TSK outputs are formed from the output of this layer; the nodes are adaptive and execute the consequences of the rules as represented by Equation (8).

$$O_{4,i} = \bar{w}_i = \bar{w}_i(p_i x + q_i y + r_i) \tag{8}$$

p_i, q_i and r_i are parameters to be learnt. These are the premise parameters. All this layer parameters (p_i, q_i, r_i) should be determined and are identified as the consequent parameters.

Layer 5: It sums all the input signals to generate the output. In this layer, there is only one node that calculates the overall output, as given by Equation (9).

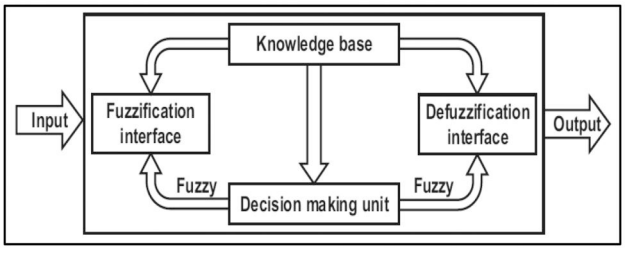


Figure 2. Fuzzy inference system.

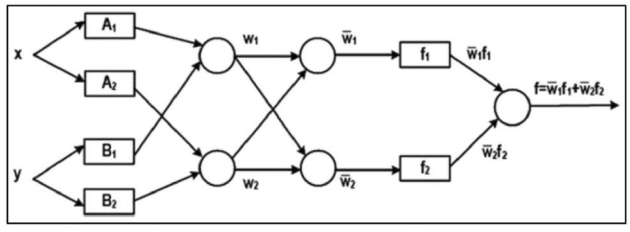


Figure 4. ANFIS architecture.

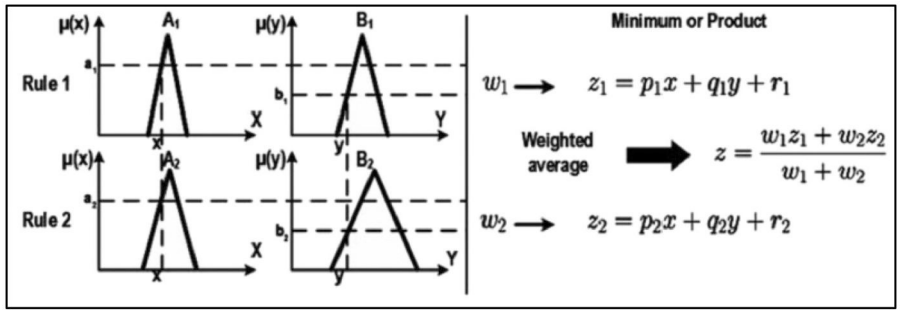


Figure 3. First-order Sugeno model.

Table 2. Optimal ANFIS performance achieved during the training phase.

N°	Input MFs	Output MF	Iterations	Number of membership functions	RMSE_Train	RMSE_Check
1	Tri	Cst	31	3 3 3 3	0.0432336	0.0672334
2	Tri	Lin	37	3 3 3 3	0.0101527	0.3228540
3	Tra	Cst	225	3 3 3 3	0.0438314	0.0663807
4	Tra	Lin	703	3 3 3 3	0.0161192	0.0574563
5	Bell	Cst	878	3 3 3 3	0.0146106	0.0250171
7	Bell	Lin	1579	3 3 3 3	0.0051974	0.0741582
8	Gauss	Cst	612	3 3 3 3	0.0318528	0.0563337
9	Gauss	Lin	378	3 3 3 3	0.0135806	0.0469595
10	Gauss2	Constant	1359	3 3 3 3	0.0133545	0.0218342
11	Gauss2	Lin	839	3 3 3 3	0.0065507	0.0853260
12	Gauss2	Constant	709	4 3 3 4	0.0121275	0.0217536
13	Gauss2	Constant	451	4 4 4 4	0.0123172	0.0217685
14	Gauss2	Constant	821	3 4 4 3	0.0130822	0.0214744
15	Gauss2	Constant	516	3 3 4 4	0.0121218	0.0216965
16	Gauss2	Constant	1500	4 4 3 3	0.0132978	0.0215965

$$O_{5,1} = \sum_i \bar{w}_i f_i = \frac{\sum_i w_i f_i}{\sum_i w_i} \tag{9}$$

The hybrid-learning algorithm proposed by Jang et al. (1997) was used for ANFIS learning in this work. This algorithm combines backpropagation and least squares estimation (LSE) to train fuzzy inference systems (Zhou et al. 2021).

Two sets of parameters are considered: premise parameters (S1) and consequent parameters (S2). S1 contains the parameters for all the selected input membership functions, while S2 contains the parameters of the output membership function (Rebouh et al. 2016).

ANFIS employs two passes for the learning algorithm:

- Forward pass: S1 is fixed and S2 is calculated using LSE.
- Backward pass: S2 is fixed and S1 is calculated using backpropagation.

The validation of the trained ANFIS model is performed using the remaining data for testing. Root mean square error (RMSE), from Equation (10), is used to assess the performance of the model (Zhou et al. 2021).

$$RMSE = \sqrt{\frac{1}{N}\sum_{i=1}^{N}\left(y_i - \hat{y}_i\right)^2} \tag{10}$$

Where N is the count of the tested data, $y_i - \hat{y}_i$ is the difference between the i^{th} desired and predicted outputs of the model, respectively.

2.2.6.2 ANFIS modeling setup. The ANFIS model, which played a crucial role in predicting the insulin release rate from hydrogel formulations, was developed based on three crucial formulation parameters: glycerol (Gly) concentration (%), propylene glycol (PG) concentration (%), and polycondensation time. These parameters directly impact the hydrogel's insulin release characteristics. The single output of the ANFIS model was dedicated to predicting the corresponding insulin release rate, providing a valuable tool for understanding the relationship between formulation parameters and drug release behavior (Figure 5).

In the creation of the ANFIS models, a systematic approach was employed. We initiated the process by collecting a comprehensive dataset encompassing the specified formulation parameters and their corresponding insulin release rates. Following the acquisition of this dataset, thorough preprocessing was applied to address missing data, outliers, and the normalization of input features. This meticulous approach ensures equal contribution of all features to the learning process, preventing discrepancies in scales and fostering faster convergence, ultimately leading to enhanced performance in machine learning models.

The selection of input features was a critical step, involving careful consideration and application of feature selection techniques to enhance the models' predictive performance. The ANFIS architecture was designed with a hybrid learning algorithm that seamlessly integrates fuzzy logic and neural networks. This architecture underwent iterative refinement, using Matlab 2018a Software, to optimize its structure for accurate predictions identification (Rebouh et al. 2016). Figure 6 depicts the evolution of training and checking errors using the RMSE formula defined in Equation (10).

For model training and validation, the experimental dataset was strategically split, allocating 90% for training the ANFIS models and reserving the remaining 10% for validation purposes. This approach

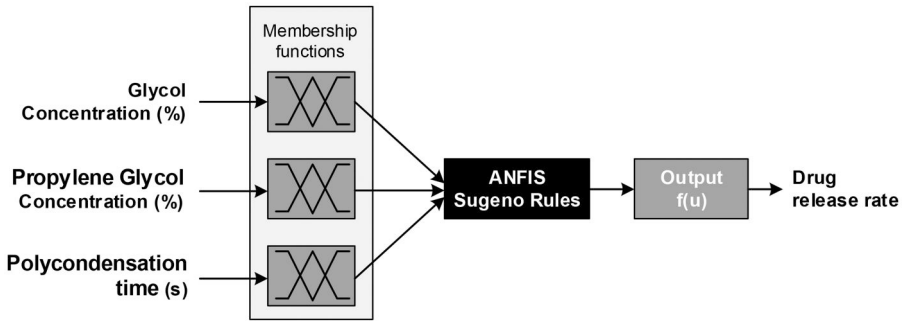


Figure 5. Studied ANFIS architecture.

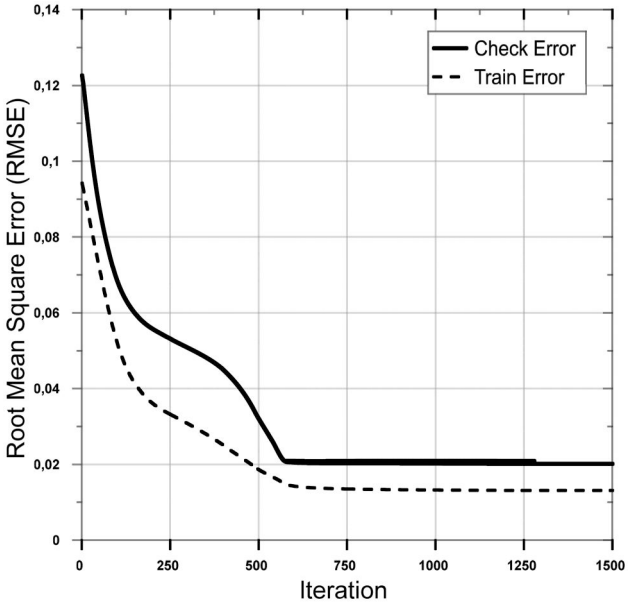


Figure 6. Evolution of training and check errors during the learning phase.

ensured that the synthesized model was effectively trained while also providing a robust evaluation of their predictive capabilities.

Performance evaluation metrics based on RMSE (Equation (10)) was employed to assess the neuro-fuzzy models' accuracy. The correlation coefficient (R^2) is also used later for the final prediction test, to evaluate the model's efficacy in capturing and explaining variance in the predicted outcomes. This comprehensive evaluation strategy ensures a thorough assessment of the model's performance across various dimensions, contributing to the robustness and validity of our findings.

2.2.6.3 Optimizing parameters for ANFIS. The core parameters optimized in developing our ANFIS models include the number of membership functions (MFs), MF type, epoch number, and the hybrid learning algorithm approach.

Various membership functions, such as trapezoidal, triangular, Gaussian, and Bell, are subjected to testing. To select the optimal number of MFs for each input, we tested from 2 to 10 MFs, evaluating the validation data fit after ANFIS training, a standard methodology as discussed in Karaboga and Kaya (2019). We selected the Gaussian MF based on its common effectiveness for prediction modeling (Talpur et al. 2017).

The tuning of the number of epochs aimed to prevent overfitting to the training data, as highlighted in reference (Walia et al. 2015). Additionally, the utilization of the hybrid learning algorithm involved a combination of both backpropagation and least squares methods in an adaptive manner. This approach has demonstrated enhanced model convergence compared to using either method alone, as mentioned in reference (Jang 1993).

The number of epochs was tuned to avoid overfitting to the training data (Walia et al. 2015). And use of the hybrid learning algorithm leveraged both backpropagation and least squares methods adaptively, which has shown improved model convergence over either method alone (Jang 1993).

Through a process of iterative model training and parameter tuning, we identified that [3 3 4 4] is an optimized combination of the number of membership functions for the ANFIS model. This configuration exhibited robust predictive capabilities. Validation metrics substantiate its strong accuracy in predicting outcomes on previously unseen test data. Based on the RMSE criteria presented in Table 2, the conclusive findings reveal that the final variant (indicated in grey in Table 2) demonstrates a significant performance superiority over the alternative configurations.

3. Results and discussions

In this section a comprehensive analysis of the obtained, experimental data including FTIR, SEM, and NMR, as well as mathematical modeling using Korsmeyer-Peppas and ANFIS approaches. This

section critically examines the influence of key formulation parameters – namely, glycerol and propylene glycol concentrations, PG/Gly ratio, and polycondensation reaction time – on the release kinetics of insulin from the developed matrix. Detailed interpretation of the results is provided to elucidate the underlying mechanisms involved in insulin release and optimize formulations to achieve a better release profile. The insights from this section further our fundamental understanding of drug release from these matrix systems and provide key knowledge to advance the formulation development.

3.1. FTIR hydrogel characterization

FTIR analysis confirmed the cross-linking reaction of the Agar-Carbomer-based hydrogel, with individual species and their cross-linked mixture spectra depicted in Figure 7. The Ag spectrum displayed characteristic peaks related to -C-O- bending and 3, 6-anhydrogalactose at 1039, 929, and 889 cm^{-1}, respectively, consistent with previous research (Sivashankari and Prabaharan 2020).

The Ca spectrum exhibited a prominent peak at 1699 cm^{-1}, attributed to C=O stretching of carboxylic groups (Zhang et al. 2018). In the synthesized hydrogel spectrum, new peaks emerged, including a broad absorption band at 3280 cm^{-1} corresponding to -OH bonds and peaks at 2978 cm^{-1} linked to C-H methyl groups of PG and Gly molecules. The peak at 1699 cm^{-1} was diminished and replaced by a peak at 1642 cm^{-1}, indicating the formation of an ester function (-CO-OR) between Ag-Ca. Additionally, an elongation of the peak at 1039 cm^{-1} indicated the formation of a -C-O- bond linking PG-Ca (Santoro et al. 2011). These results demonstrate the successful chemical crosslinking of the Ag-Ca hydrogel in the presence of PG and Gly.

3.2. SEM analysis

The choice of crosslinking method, particularly microwave-assisted polycondensation, has a significant impact on hydrogel morphology and crosslinking stability. These findings are highly relevant and provide valuable insights for optimizing hydrogel synthesis in the pharmaceutical industry.

Microstructural properties of hydrogels were analyzed using scanning electron microscopy (SEM). In Figure 8(a,b), two hydrogels with the same polymer and crosslinking agent amounts were compared. The first (in Figure 8(a), was produced with microwave-assisted polycondensation, while the second (in Figure 8(b) followed conventional methods without

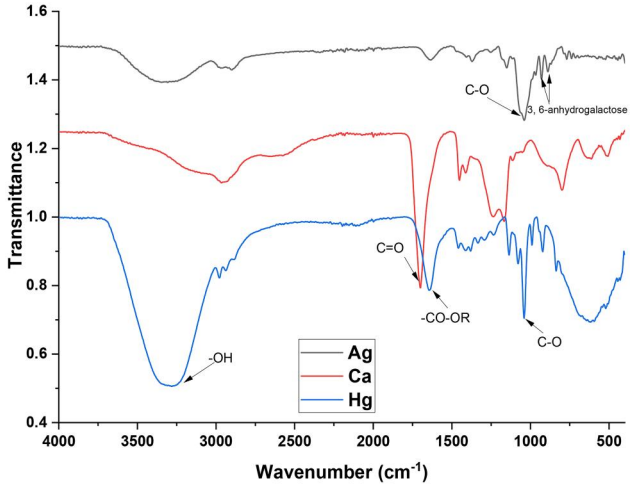


Figure 7. FTIR spectra of Agar (Ag), Carbomer (Ca) and the Ag-Ca-based hydrogel (Hg).

microwave exposure. Significant differences in microstructure were observed. Figure 8(a) displayed a compact, tightly linked network, indicating a uniform and interconnected structure. In contrast, Figure 8(b) revealed a porous network with voids, suggesting a less extensively linked structure. When a single crosslinking agent was used (Figure 8(c)), an open, porous network was evident, implying a less densely interwoven structure. Furthermore, Figure 8(d) displayed SEM images of a hydrogel prepared without crosslinking agents, showing dispersed polymers in a fused state without forming a cohesive network (Baysal et al. 2013).

3.3. NMR analysis

The H1-NMR analysis was carried out to prove that the hydrogel was successfully crosslinked. The results of the H1 NMR analysis are illustrated by the spectra of Figure 9.

The spectra in Figure 9(a,b) represent two polymers, Carbomer and Agarose, respectively. Figure 9(b,c) display the spectra of the crosslinking system with Propylene glycol and Glycerol, separately. Both spectra show a peak around 4.7 ppm, corresponding to the anomeric proton of deuterium oxide (D_2O) (Sara et al. 2020). The H1NMR spectrum of the hydrogels formed by combining Agarose and Carbomer is characterized by wide signals due to dipole-dipole coupling. The spectrum of the cross-linked hydrogel F8 (Figure 9(e)) shows characteristic peaks: Peaks at 1,126 and 1,577 ppm correspond to aliphatic protons and methyl protons (CH_2), respectively. The chemical shift of the proton related to the acetyl group (R-C=O) is observed at 2,216 ppm. Peaks at 3.425 and 3.507 ppm are typical for protons near electronegative atoms such

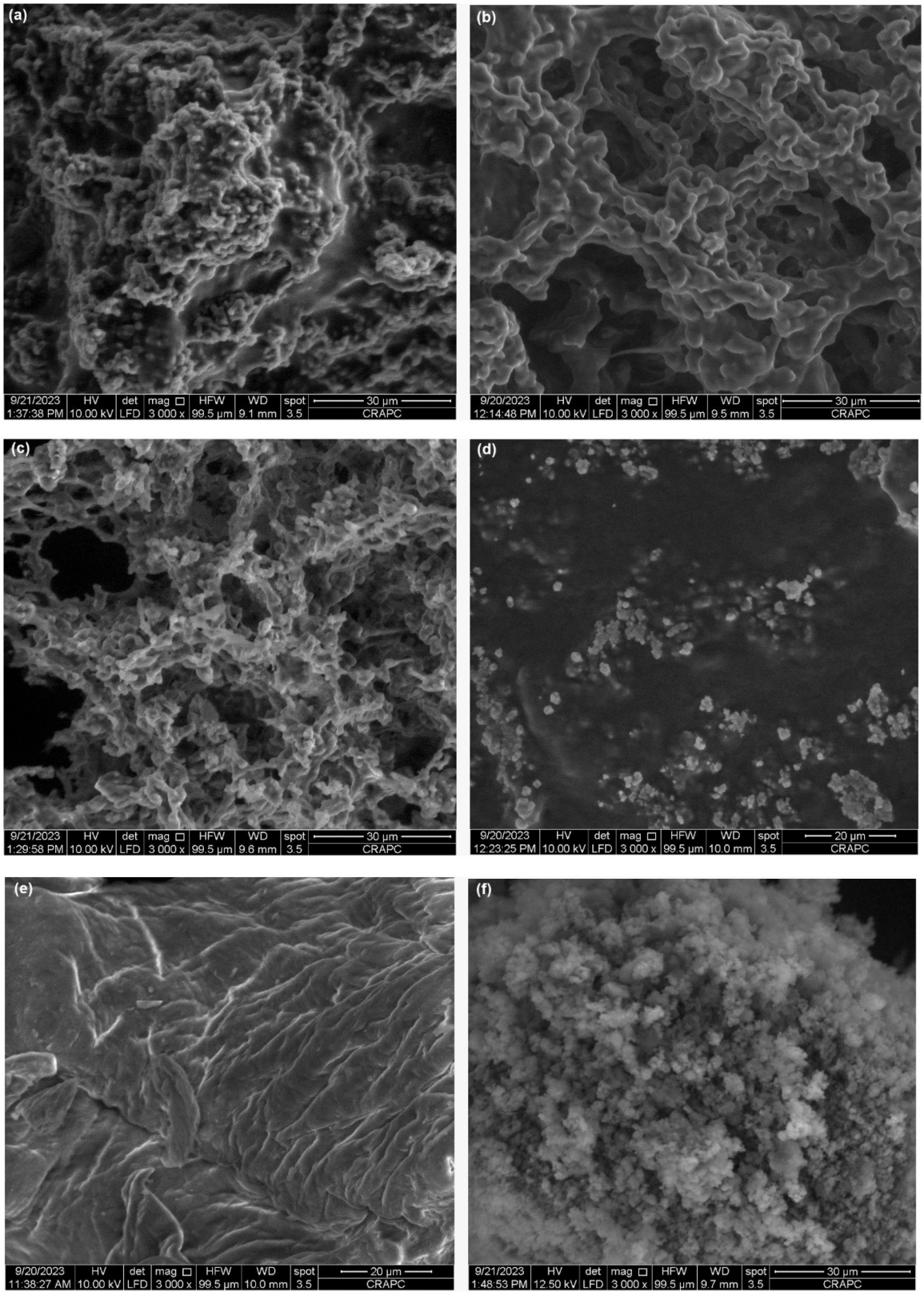


Figure 8. (a) 1r/Carbomer hydrogel exposed to polycondensation assisted by microwave; (b) crosslinked Agar/Carbomer hydrogel without microwave exposure; (c) hydrogel with a single crosslinking agent; (d) hydrogel without crosslinking agents; (e) Agar; (f) Carbomer.

as oxygen, related to protons in multiple hydroxyl groups (HO-). New peaks around 3,760 ppm and 4,106 ppm in the spectrum are associated with the ester function (-(C=O)-O-). The appearance of peaks in the 3,760 ppm and 4,106 ppm region indicates the formation of an ester function (-(C=O)-O-). This suggests

that the carboxyl group (–C(O)OH) of Carbomer has been connected with the Hydroxyl group (HO-) of Agarose, forming the ester function. This is shown in Figure 9. The successful formation of the ester function indicates the crosslinking of the hydrogel. Comparing with Previous Research, the results align with findings from Santoro et al. (2011), indicating the consistency of the observed peaks and the successful crosslinking of the hydrogel.

By combining this information, the chemical structure of the elaborated cross-linked hydrogel macromolecule can be provided in Figure 10.

3.4. Kinetic release profile and modeling

An *in vitro* study was conducted to analyze the drug release of insulin-loaded Ag/Ca-based hydrogels prepared by polycondensation in PBS at 37 °C. The impact

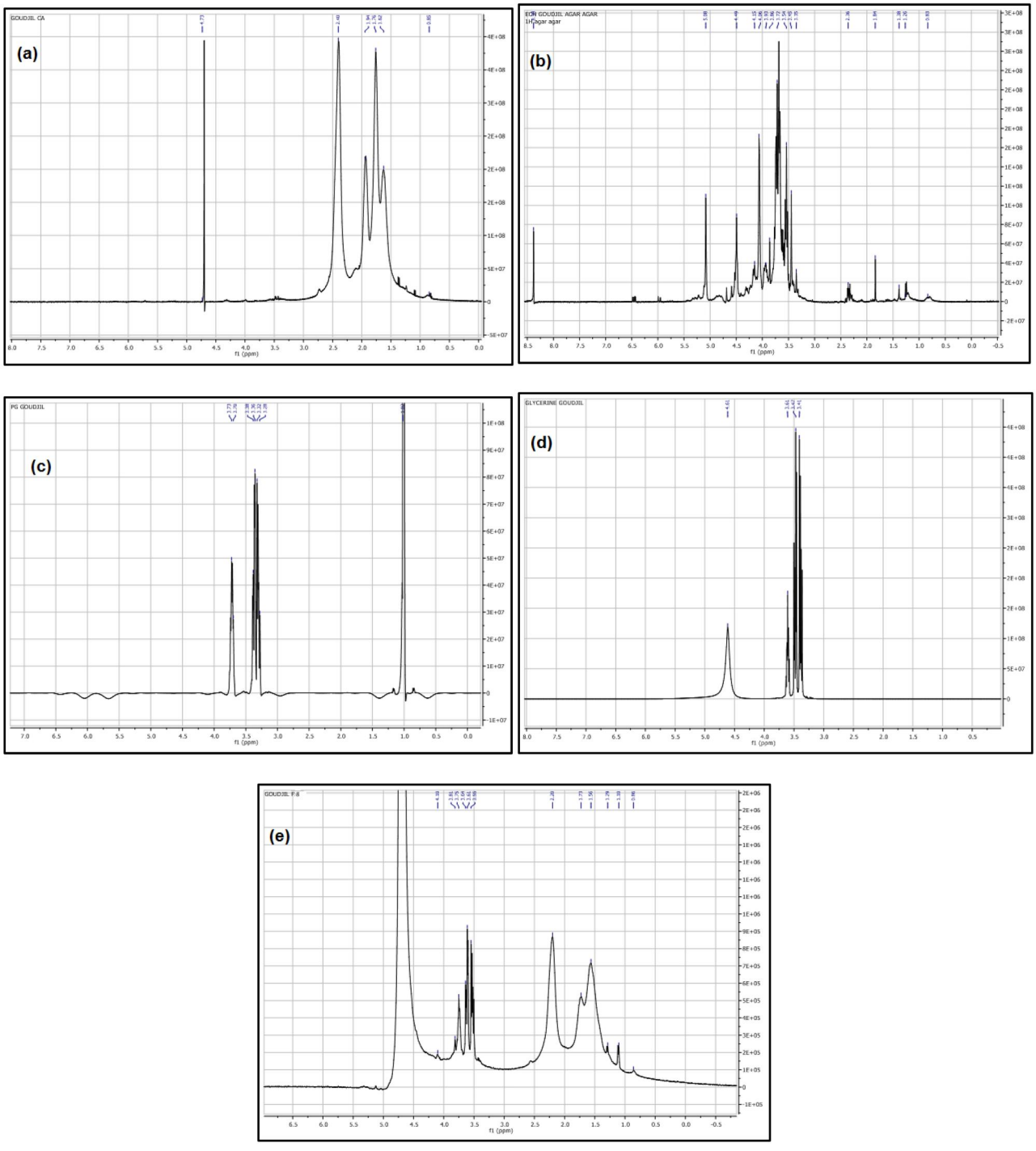


Figure 9. NMR spectra: (a) Carbomer; (b) Agar; (c) propylen glycol; (d) glycerol; (e) hydrogel F8.

of PG and Gly concentrations, along with the polycondensation time was also investigated. The experimental results presented in Figure 11 clearly show that the fastest release was observed in hydrogel F1.

In fact, this formulation did not contain Gly and was not subjected to microwave irradiation, and consequently there was no polycondensation reaction (no hydrogen bonding with Ca). Hydrogels created without any added PG – F2 to F4 – displayed comparable trends to F1, with a release time between 6.5 and 7.5 h, depending on the concentration of Gly and the polycondensation time. In contrast, hydrogels F5-F7 that do not contain Gly, but contain 30% PG, have shown extended-release profiles of over 7.5–8.5 h, which increase with increasing polycondensation time, indicating the formation of ester bonds. In addition, it should be noted that all of the above formulations showed a burst release in the first 30 min, which may be due to the insufficient amount of PG/Gly cross-linking agents to form strong hydrogels capable of retaining drugs through their cross-linked networks (Lefnaoui and Moulai-Mostefa 2014). Furthermore, a higher rate of drug release was observed in formulations containing only Gly, as its characteristics enable a rapid release of drugs (Lefnaoui and Moulai-Mostefa 2014).

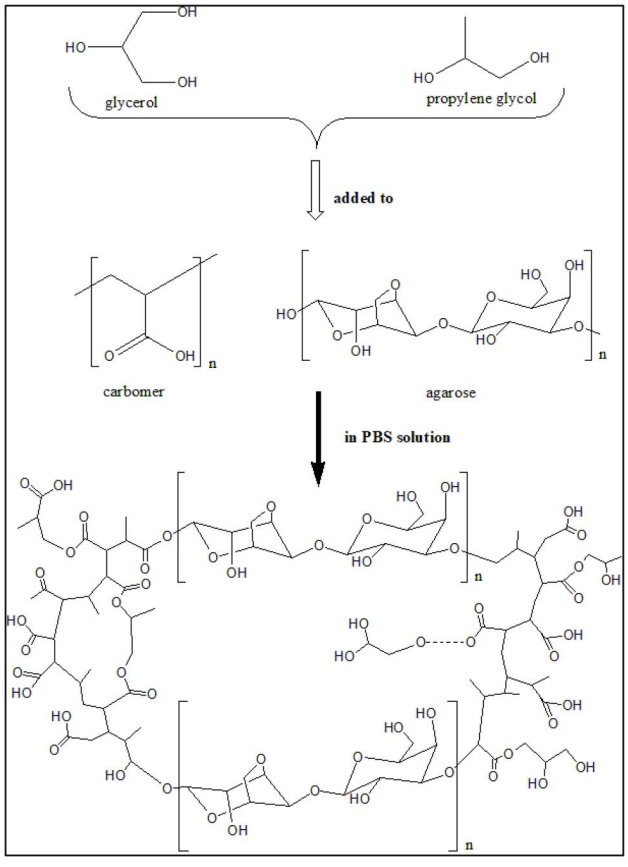


Figure 10. Chemical structures pattern of the crosslinking reaction.

3.4.1. Korsmeyer-Peppas modeling results

The release kinetics of all formulations adhere to the Korsmeyer-Peppas model with a correlation coefficient between 0.95 and 0.99, as stated in Table 3. This indicates that the primary release mechanism is controlled by diffusion and relaxation.

Previous studies have demonstrated that drug release is controlled by diffusion when the value of n equals 0.43, while a value of 0.85 indicates control by swelling (Siepmann and Peppas 2012). In this study, as long as the values of n for the formulated hydrogels range between 0.43 and 0.85, drug release is conducted by the concurrent phenomena of diffusion and relaxation (anomalous transport).

3.4.2. ANFIS modeling results

Concerning the ANFIS modelling performance, it appears that the ANFIS model adeptly predicted the insulin release rate, as demonstrated by the substantial concordance between the experimental and predicted values depicted in Figure 11.

3.5. Formulation parameters effect

3.5.1. Effect of the glycerol concentration on the insulin release kinetic

Figure 12 demonstrates that, with a consistent polycondensation time and PG concentration, F5 without Gly exhibited the fastest release of insulin (7.5 h), accompanied by a burst release effect within the first hour. Nevertheless, the hydrogels F8 (1%) and F11

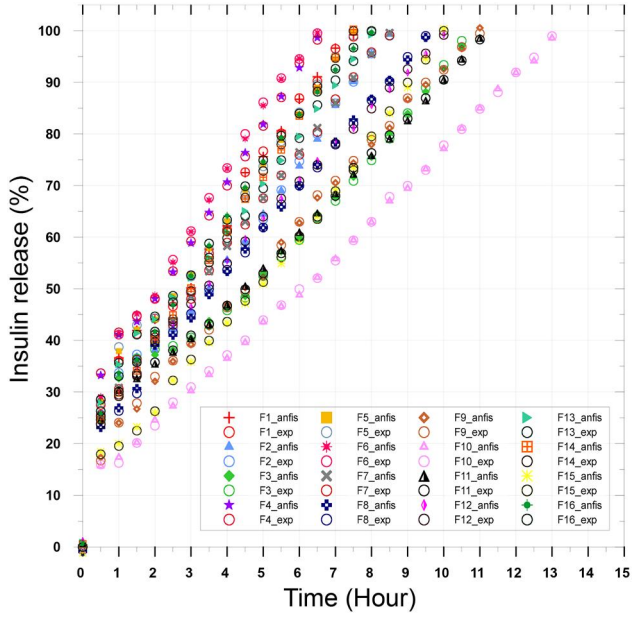


Figure 11. Insulin release kinetics profiles from the different hydrogel formulas (experimental and predicted results) in PBS 7.4 at 37 °C.

Table 3. Korsmeyer-Peppas modeling results.

	Korsmeyer Peppas kinetic model			
Formula number	k	n	R^2	Insulin release mechanism
F01	33.97	0.49	0.97	Anomalous transport
F02	30.61	0.49	0.97	Anomalous transport
F03	28.85	0.44	0.95	Anomalous transport
F04	39.96	0.43	0.97	Anomalous transport
F05	35.20	0.46	0.98	Anomalous transport
F06	37.99	0.49	0.99	Anomalous transport
F07	30.46	0.51	0.98	Anomalous transport
F08	27.41	0.53	0.98	Anomalous transport
F09	22.21	0.60	0.99	Anomalous transport
F10	17.16	0.62	0.98	Anomalous transport
F11	27.41	0.47	0.97	Anomalous transport
F12	29.68	0.49	0.99	Anomalous transport
F13	34.50	0.46	0.98	Anomalous transport
F14	29.18	0.57	0.98	Anomalous transport
F15	19.74	0.64	0.97	Anomalous transport
F16	32.12	0.52	0.99	Anomalous transport

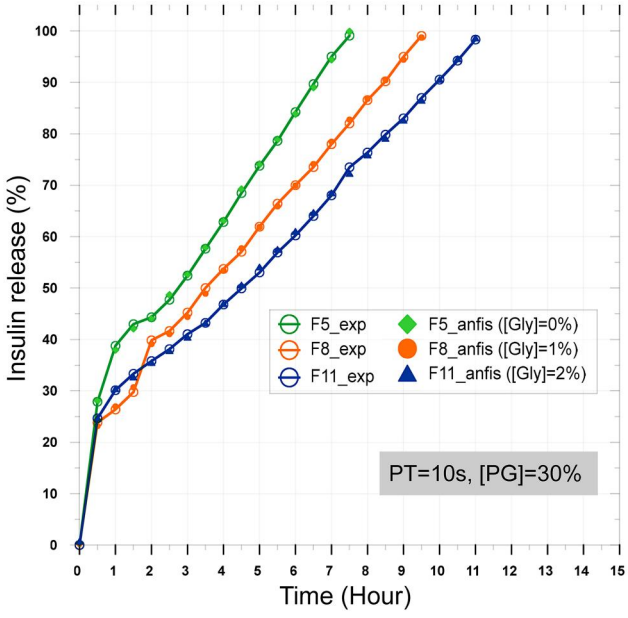


Figure 12. Effect of the glycerol concentration on the insulin release kinetic (experimental and predicted results).

(2%) showed prolonged release by the gradual addition of Gly, with release periods of 9.5 and 11 h, respectively.

3.5.2. Effect of the propylene glycol concentration

In this part of study, the polycondensation time and the Gly concentration were kept constant while the PG concentration was varied and the release results are shown in Figure 13. The hydrogel formulation (F8), comprising 30% PG, exhibited a longer release of insulin over a period of 9.5 h compared to the hydrogel with no PG added (F2), which took 8.5 h to release insulin. However, the hydrogel formula with an excessive amount of PG (F14) exhibited similar behavior to the hydrogel formula without PG (F2). This suggests that an excess of PG may have an adverse effect on the release properties of Agar-Carbomer-based hydrogels.

3.5.3. Effect of the PG/Gly ratio

The PG/Gly ratio represents the concentration variation of both PG and Gly. By fixing the polycondensation time, we can analyze the impact of different PG/Gly ratios on insulin release. Figure 14 presents the results obtained. It has been demonstrated that F4, which doesn't contain PG but only Gly (2%), gave the fastest release of insulin in 6.5 h. It seems that formulation 15, which had no PG and only 2% Gly, gave the fastest release of insulin, while formulations 13 (with 60% PG and no Gly) and 16 (with the maximum levels of both PG and Gly) showed similar release profiles but reached the total amount of drug released in 8 h, which cannot be considered as sustained release.

3.5.4. Effect of the polycondensation time

The polycondensation time was varied while keeping the concentrations of PG and Gly fixed, and the increased release of insulin was observed. Figure 15 demonstrates that the polycondensation time greatly affects the release profile. Specifically, F10 (crosslinked with 30% PG, 1% Gly, and subjected to 30 s of microwaves irradiation) released insulin over a longer period compared to F8 and F9, which were crosslinked for 10 and 20 s, respectively, and had identical crosslinking agent proportions. The insulin release time increased with increasing polycondensation time, with F8, F9 and F10 providing release times of 9.5, 11 and 13 h respectively.

The findings suggest that formulations with insufficient PG/Gly crosslinkers exhibited burst release and

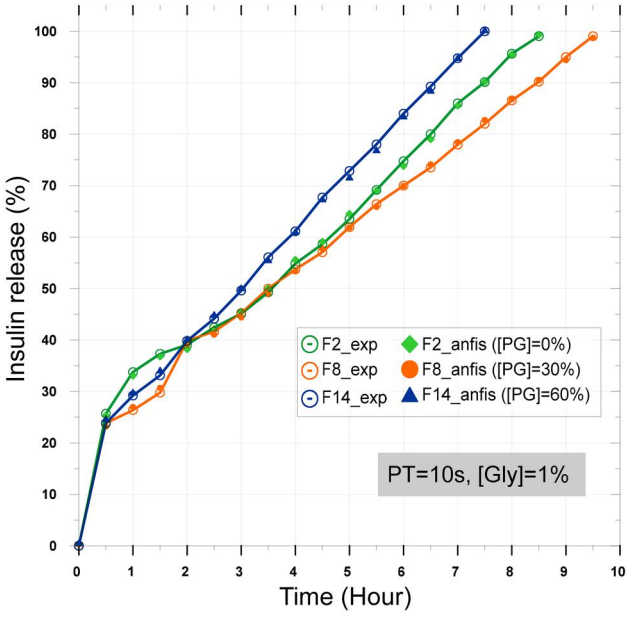


Figure 13. Effect of the propylene glycol concentration on the insulin release kinetic (experimental and predicted results).

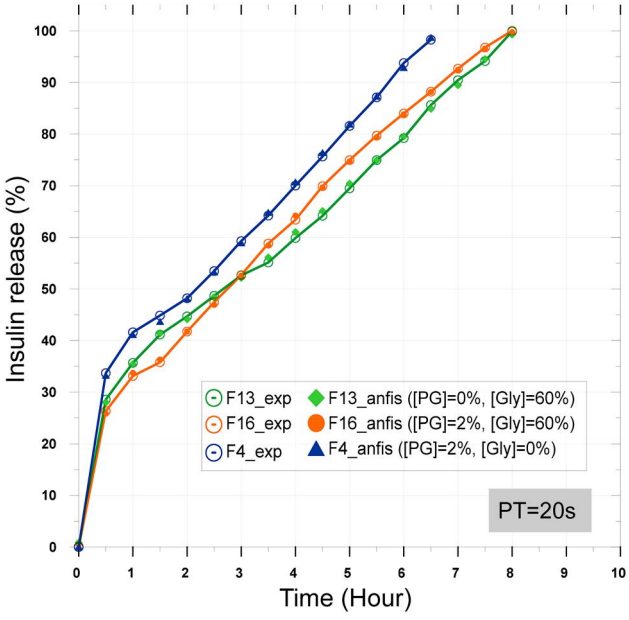


Figure 14. Effect of the proportion of cross-linking agents on the insulin release kinetic (experimental and predicted results).

weak hydrogel formation. Gly alone facilitated higher rates of drug release during the burst effect, owing to its inherent ability to allow prompt drug release (Lefnaoui and Moulai-Mostefa 2014). Moreover, a brief polycondensation reaction time thwarted the formation of hydrogen bonds with Ca.

An enhancement in drug release profiles was noted by increasing PG and Gly concentrations simultaneously up to 30 and 1%, respectively, showing sustained release over time. Formula F10, which comprised moderate amounts of PG and Gly and

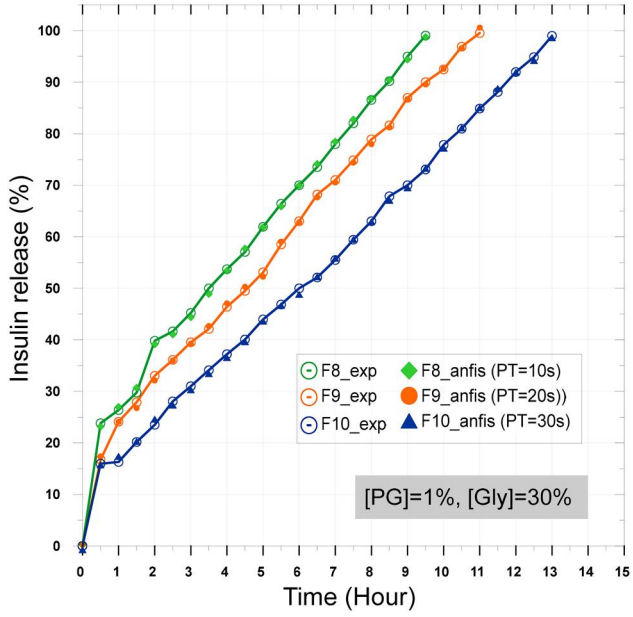


Figure 15. Effect of the polycondensation time on the insulin release kinetic (experimental and predicted results).

was allowed a maximum polycondensation time of 30 s, displayed the longest release time of 13 h. The strong crosslinking characteristics of the hydrogel allowed for a more pronounced controlled release of insulin from F8. This was facilitated by sufficient condensation time, which provided high irradiation energy and facilitated efficient crosslinking without adding additional Gly and PG (Maitra and Shukla 2014).

When surplus amounts of PG and Gly were integrated into hydrogel formulation (F16), they exhibited similar behavior to those with insufficient amounts of cross-linking agents. This is probably due to the fact that an excess of cross-linking agents can lead to the formation of denser network structures, which can result in unstable gels (Siepmann and Peppas 2012; He et al. 2017).

3.6. ANFIS prediction of the formulation parameters effect

The ANFIS model, as demonstrated in Figures 12–15, is capable of predicting the impact of formulation parameters on insulin release kinetics. This model allows for the consideration of various factors influencing insulin release, including the composition of the drug delivery system.

Researchers can leverage the ANFIS model to simulate different scenarios and forecast the effects of adjusting formulation parameters on insulin release. This is

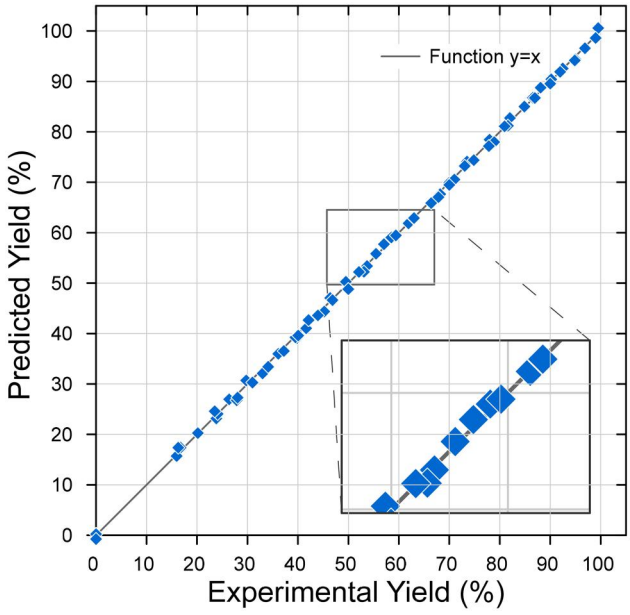


Figure 16. Point cloud representing the ANFIS predicted release amount as a function of the experimental data.

particularly valuable in developing drug delivery systems to identify optimal formulations for controlled and sustained insulin delivery. A high-performing hydrogel derived from the Fuzzy Takagi-Sugeno model is suitable for inhalation delivery.

The reliability of the ANFIS model depends on the quality and quantity of the training data, so selecting high-quality data and appropriate features is crucial to ensure accurate predictions.

3.7. ANFIS predicted insulin release amount as a function of the experimental data

Figure 16 shows the correlation plot of the predicted release rate against the experimental release rate. It is evident that the data points cloud is very close to the first bisector, which indicates the reliability and excellent performance of the ANFIS model, as shown by the narrow gap between the experimental and predicted values. To comprehensively assess the accuracy and reliability of the ANFIS model, a correlation coefficient and root mean squared error were calculated. The achieved results indicate that the model performed very well with a high correlation coefficient close to unity (R^2=0.9999) and an RMSE of 2.159×10^{-2}. This signifies the successful development of a high-quality ANFIS model.

The neuro-fuzzy model was established based on the parameters used in this particular study. However, other relevant factors, such as insulin concentration, are not taken into account. On the other hand, the model relies on three input characteristics: crosslinking agent's concentrations, polycondensation time, and release. If these characteristics are not measured accurately, the model predictions may be limited or inaccurate. The properties of hydrogels can change over time due to various environmental factors. The model may not account for these dynamic changes, leading to discrepancies between predicted and actual insulin release kinetics in real-world scenarios. The study mentions an excellent correlation with experimental data, but experimental conditions may exhibit inherent variability. In the future, the study needs to address the long-term stability of hydrogel formulations and their impact on insulin release. This is particularly important for extended drug delivery applications.

4. Conclusion

The comprehensive nature of this study significantly advances our understanding of hydrogel synthesis and provides invaluable insights into its potential applications in diabetes treatment. Our research involved the development of an ANFIS model specifically designed to predict insulin release from Ag-Ca based hydrogels. This model takes into account crucial factors such as cross-linking reagent concentration and polycondensation time, ensuring a high level of accuracy in its predictions.

To validate the success of the polycondensation reaction, we employed FTIR spectroscopy, carefully monitoring the appearance and disappearance of specific peaks indicating the formation of an ester function (-CO-OR) between Ag-Ca and a -C-O- bond linking PG-Ca. This result confirms the successful chemical crosslinking of the Ag-Ca hydrogel in the presence of PG and Gly. Further, our study delved into the impact of various polycondensation techniques on hydrogel microstructure through comprehensive SEM analysis. The SEM examination of hydrogel microstructures, comparing microwave-assisted polycondensation with conventional methods, demonstrated that the former yielded a dense, closely connected network, while the latter generated a porous network with voids. Additionally, utilizing a single crosslinking agent resulted in an open, porous structure, whereas hydrogels without crosslinking agents showed dispersed polymers fused together without forming a cohesive network. In addition, the NMR analysis provide evidence for the successful crosslinking of hydrogels formed by combining Carbomer and Agarose, as indicated by the appearance of characteristic peaks associated with the ester function. The results are in agreement with previous research by M. Santoro.

Hydrogels containing insulin were synthesized and subjected to *in vitro* drug release testing using HPLC. The release rate within Agar-Carbomer-based hydrogels was found to be influenced by parameters such as PG and Gly concentrations, irradiation, and polycondensation. Notably, Hydrogel F8 comprising 30% PG has exhibited robust crosslinking properties, resulting in a sustained release profile with a longer release of insulin over a period of 9.5 h. The drug release mechanism aligned well with the Korsmeyer-Peppas model, but our findings suggest the potential applicability of a more sophisticated model for a more nuanced understanding.

Our ANFIS modeling proved highly successful in predicting insulin release, achieving an exceptional level of accuracy with an R^2 value of 0.9999 and an RMSE of 2.159×10^{-2}. This underscores the reliability and precision of neuro-fuzzy modeling in the context of drug release from hydrogels. This study not only emphasizes the potential of ANFIS modeling but also showcases its utility in simulating the effects of various hydrogel compositions and properties.

In conclusion, our research contributes significantly to the field of drug delivery systems and biomedical engineering by highlighting the potential of neuro-fuzzy modeling. The detailed exploration of hydrogel synthesis, coupled with the accurate prediction capabilities of our ANFIS model, opens new avenues for the development of targeted and efficient drug delivery systems, particularly in the context of diabetes treatment.

Disclosure statement

The authors declare that they have no conflict of interest.

Funding

This work is supported by the Directorate General for Scientific Research and Technological Development (DGRSDT) of the Algerian Ministry of Higher Education and Scientific Research (MESRS).

References

Abba SI, Pham QB, Usman AG, Linh NTT, Aliyu DS, Nguyen Q, Bach Q-V. 2020. Emerging evolutionary algorithm integrated with kernel principal component analysis for modeling the performance of a water treatment plant. J Water Process Eng. 33:101081. doi: 10.1016/j.jwpe.2019.101081.

Alsarra IA, Hamed AY, Mahrous GM, El Maghraby GM, Al-Robayan AA, Alanazi FK. 2009. Mucoadhesive polymeric hydrogels for nasal delivery of acyclovir. Drug Dev Ind Pharm. 35(3):352–362. doi: 10.1080/03639040802360510.

Baghban Taraghdari Z, Imani R, Mohabatpour F. 2019. A review on bioengineering approaches to insulin delivery: a pharmaceutical and engineering perspective. Macromol Biosci. 19(4):1800458.

Baysal K, Aroguz AZ, Adiguzel Z, Baysal BM. 2013. Chitosan/alginate crosslinked hydrogels: preparation, characterization and application for cell growth purposes. Int J Biol Macromol. 59:342–348. doi: 10.1016/j.ijbiomac.2013.04.073.

Benyezza H, Bouhedda M, Kara R, Rebouh S. 2023. Smart platform based on IoT and WSN for monitoring and control of a greenhouse in the context of precision agriculture. Int Things. 23:100830. doi: 10.1016/j.iot.2023.100830.

Benyezza H, Bouhedda M, Rebouh S. 2021. Zoning irrigation smart system based on fuzzy control technology and IoT for water and energy saving. J Clean Prod. 302:127001. doi: 10.1016/j.jclepro.2021.127001.

Boscari F, Avogaro A. 2021. Current treatment options and challenges in patients with type 1 diabetes: pharmacological, technical advances and future perspectives. Rev Endocr Metab Disord. 22(2):217–240. doi: 10.1007/s11154-021-09635-3.

Bouhedda M, Lefnaoui S, Rebouh S, Yahoum MM. 2019. Predictive model based on adaptive neuro-fuzzy inference system for estimation of cephalexin adsorption on the octenyl succinic anhydride starch. Chemomet Int Lab Sys. 193:103843. doi: 10.1016/j.chemolab.2019.103843.

Collins DS, Sánchez-Félix M, Badkar AV, Mrsny R. 2020. Accelerating the development of novel technologies and tools for the subcutaneous delivery of biotherapeutics. J Controlled Rel. 321:475–482. doi: 10.1016/j.jconrel.2020.02.036.

Crasto W, Jarvis J, Davies MJ. "Handbook of insulin therapies," 2016.

Dadkhah MR, et al. 2017. Prediction of solubility of solid compounds in supercritical CO2 using a connectionist smart technique. J Supercrit Fluids. 120:181–190.

Elbeltagi A, Jaiswal RK, Galkate RV, Kumar M, Lohani AK, Tyagi J. 2023. Modeling soil water retention under different pressures using adaptive neuro-fuzzy inference system. Water Resour Manage. 37(4):1519–1538. doi: 10.1007/s11269-023-03439-7.

Elshaarani, Tarig, Yu, Haojie, Wang, Li, Ullah, Raja Summe, Haroon, Muhammad, Khan, Rizwan Ullah, Fahad, Shah, Khan, Amin, Nazir, Ahsan, Usman, Muhammad, et al., "Synthesis of hydrogel-bearing phenylboronic acid moieties and their applications in glucose sensing and insulin delivery J Mater Chem B, vol. 6, no. 23, pp. 3831–3854, 2018. doi: 10.1039/c7tb03332j.

European Pharmacopoeia: 8.0. 2014. Council of Europe. https://www.edqm.eu/en/d/259169.

He G, et al. 2017. Preparation and properties of quaternary ammonium chitosan-g-poly (acrylic acid-co-acrylamide) superabsorbent hydrogels. React Funct Polym. 111:14–21.

Hezaveh H, Muhamad II, Noshadi I, Shu Fen L, Ngadi N. 2012. Swelling behaviour and controlled drug release from cross-linked $κ$-carrageenan/NaCMC hydrogel by diffusion mechanism. J Microencapsul. 29(4):368–379. doi: 10.3109/02652048.2011.651501.

Hoare TR, Kohane DS. 2008. "Hydrogels in drug delivery : progress and challenges" Polymers with aligned carbon nanotubes: active composite materials. Polymer. 49(8):1993–2007. doi: 10.1016/j.polymer.2008.01.027.

Huang ZJ, Hahn J. 2009. Fuzzy modeling of signal transduction networks. Chem Eng Sci. 64(9):2044–2056. doi: 10.1016/j.ces.2009.01.041.

Jang J-SR, Sun C-T, Mizutani E. 1997. Neuro-fuzzy and soft computing-a computational approach to learning and machine intelligence [Book Review]. IEEE Trans Automat Contr. 42(10):1482–1484.

Jang JSR. 1993. ANFIS: adaptive-network-based fuzzy inference system. IEEE Trans Syst Man Cybern. 23(3):665–685. doi: 10.1109/21.256541.

Jarosinski MA, Dhayalan B, Chen Y-S, Chatterjee D, Varas N, Weiss MA. 2021. Structural principles of insulin formulation and analog design: a century of innovation. Mol Metab. 52: 101325. doi: 10.1016/j.molmet.2021.101325.

Kankala RK, Lin X-F, Song H-F, Wang S-B, Yang D-Y, Zhang YS, Chen A-Z. 2018. Supercritical fluid-assisted decoration of nanoparticles on porous microcontainers for codelivery of therapeutics and inhalation therapy of diabetes. ACS Biomater Sci Eng. 4(12):4225–4235. doi: 10.1021/acsbiomaterials.8b00992.

Karaboga D, Kaya E. 2019. Adaptive network based fuzzy inference system (ANFIS) training approaches: a comprehensive survey. Artif Intell Rev. 52(4):2263–2293. doi: 10.1007/s10462-017-9610-2.

Kaur K, Jindal R, Jindal D. 2018. RSM-CCD optimized microwave-assisted synthesis of chitosan and gelatin-based pH sensitive, inclusion complexes incorporated hydrogels and their use as controlled drug delivery systems. J Drug Deliv Sci Technol. 48:161–173.

Korsmeyer RW, Gurny R, Doelker E, Buri P, Peppas NA. 1983. Mechanisms of solute release from porous hydrophilic polymers. Int J Pharm. 15(1):25–35.

Kumar S. 2020. Estimation capabilities of biodiesel production from algae oil blend using adaptive neuro-fuzzy inference system (ANFIS). Energy Sources Part A. 42(7): 909–917. doi: 10.1080/15567036.2019.1602203.

Kumbhar KP, Suryawanshi SS, Patil SV. 2022. Novel route of inhaled insulin for diabetes treatment. AJPT. 12(1): 25–32. doi: 10.52711/2231-5713.2022.00005.

Lefnaoui S, Moulai-Mostefa N, Faculty of Sciences and Technology, University of Medea, 26001 Medea, Algeria. 2013. Investigation of the effects of cellulose derivatives on the kinetics of drug release from cellulose-based hydrogel using a response surface method. JPTRM. 1(1): 119–132. doi: 10.15415/jptrm.2013.11008.

Lefnaoui S, Moulai-Mostefa N. 2014. Investigation and optimization of formulation factors of a hydrogel network based on kappa carrageenan–pregelatinized starch blend using an experimental design. Colloids Surf A Physicochem Eng Asp. 458:117–125.

Maitra J, Shukla VK. 2014. Cross-linking in hydrogels – a review. Am J Polym Sci. 4(2):25–31.

Mansoor S, Kondiah PPD, Choonara YE. 2021. Advanced hydrogels for the controlled delivery of insulin. Pharmaceutics. 13(12):2113. doi: 10.3390/pharmaceutics13122113.

Mathieu C, Pieter-Jan M, Roman V. 2021. One hundred years of insulin therapy. Nature Rev. 17:715–725.

Owens DR, Zinman B, Bolli G. 2003. Alternative routes of insulin delivery. Diabetic Med. 20(11):886–898. doi: 10.1046/j.1464-5491.2003.01076.x.

Parhi R. 2017. Cross-linked hydrogel for pharmaceutical applications : a review. Tabriz Univ Med Sci. 7:515–530.

Pramanik S, Mohanto S, Manne R, Rajendran RR, Deepak A, Edapully SJ, Patil T, Katari O. 2021. Nanoparticle-based drug delivery system: the magic bullet for the treatment of chronic pulmonary diseases. Mol Pharm. 18(10): 3671–3718. doi: 10.1021/acs.molpharmaceut.1c00491.

Rebouh S, Bouhedda M, Hanini S. 2016. Neuro-fuzzy modeling of Cu(II) and Cr(VI) adsorption from aqueous solution by wheat straw. Desalination Water Treat. 57(14):6515–6530. doi: 10.1080/19443994.2015.1009171.

Rebouh S, Lefnaoui S, Bouhedda M, Yahoum MM, Hanini S. 2019. Neuro-fuzzy modeling of ibuprofen-sustained release from tablets based on different cellulose derivatives. Drug Deliv Transl Res. 9(1):162–177. doi: 10.1007/s13346-018-00592-0.

Salawi A, Khan A, Zaman M, Riaz T, Ihsan H, Butt MH, Aman W, Khan R, Majeed I, Almoshari Y, et al. 2022. Development of statistically optimized chemically cross-linked hydrogel for the sustained-release delivery of favipiravir. Polymers (Basel). 14(12):2369. doi: 10.3390/polym14122369.

Santoro M, Marchetti P, Rossi F, Perale G, Castiglione F, Mele A, Masi M. 2011. Smart approach to evaluate drug diffusivity in injectable agar-carbomer hydrogels for drug delivery. J Phys Chem B. 115(11):2503–2510. doi: 10.1021/jp1111394.

Sara H, Yahoum MM, Lefnaoui S, Abdelkader H, Moulai-Mostefa N. 2020. New alkylated xanthan gum as amphiphilic derivatives: synthesis, physicochemical and rheological studies. J Mol Struct. 1207:127768.

Siepmann J, Peppas NA. 2012. Modeling of drug release from delivery systems based on hydroxypropyl methylcellulose (HPMC). Adv Drug Deliv Rev. 64:163–174.

Sivashankari PR, Prabaharan M. 2020. Three-dimensional porous scaffolds based on agarose/chitosan/graphene oxide composite for tissue engineering. Int J Biol Macromol. 146: 222–231. doi: 10.1016/j.ijbiomac.2019.12.219.

Takagi T, Sugeno M. 1985. Fuzzy identification of systems and its applications to modeling and control. IEEE Trans Syst Man Cybern. SMC-15(1):116–132.

Talpur N, Salleh MNM, Hussain K. 2017. "An investigation of membership functions on performance of ANFIS for solving classification problems" IOP Conf. Ser.: mater. Sci. Eng. 226: 012103. doi: 10.1088/1757-899X/226/1/012103.

Walia N, Singh H, Sharma A. 2015. ANFIS: adaptive neuro-fuzzy inference system-a survey. Int J Comput Appl. 123(13):32–38. doi: 5120/ijca2015905635.

Zarei K, Taheri F. 2016. Prediction of solubility of some statin drugs in supercritical carbon dioxide using classification and regression tree analysis and adaptive neuro-fuzzy inference systems. Russ Chem Bull. 65(4):1131–1138. doi: 10.1007/s11172-016-1424-x.

Zhang X, Gu X, Wang X, Wang H, Mao S. 2018. Tunable and sustained-release characteristics of venlafaxine hydrochloride from chitosan–carbomer matrix tablets based on in situ formed polyelectrolyte complex film coating. Asian J Pharm Sci. 13(6):566–574. doi: 10.1016/j.ajps.2018.01.004.

Zhou J, Li C, Arslan CA, Hasanipanah M, Bakhshandeh Amnieh H. 2021. Performance evaluation of hybrid FFA-ANFIS and GA-ANFIS models to predict particle size distribution of a muck-pile after blasting. Eng Comput. 37:265–274.